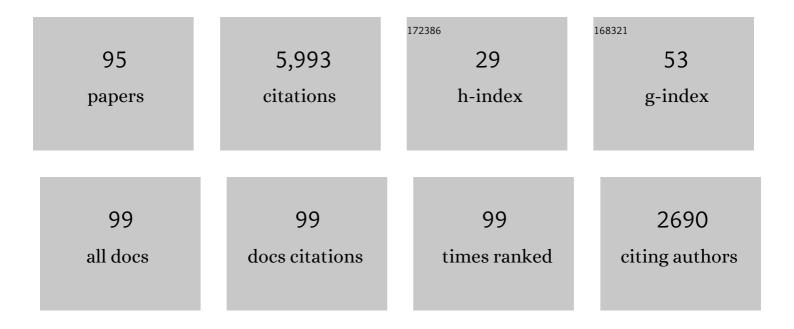
Ian A Sigal

List of Publications by Year in descending order

Source: https://exaly.com/author-pdf/2773355/publications.pdf Version: 2024-02-01



#	Article	IF	CITATIONS
1	Lamina cribrosa vessel and collagen beam networks are distinct. Experimental Eye Research, 2022, 215, 108916.	1.2	7
2	Real-time imaging of optic nerve head collagen microstructure and biomechanics using instant polarized light microscopy. Experimental Eye Research, 2022, 217, 108967.	1.2	13
3	A high-accuracy and high-efficiency digital volume correlation method to characterize in-vivo optic nerve head biomechanics from optical coherence tomography. Acta Biomaterialia, 2022, 143, 72-86.	4.1	12
4	A Workflow for 3D Reconstruction and Quantification of the Monkey Optic Nerve Head Vascular Network. Journal of Biomechanical Engineering, 2022, , .	0.6	0
5	Eye-specific 3D modeling of factors influencing oxygen concentration in the lamina cribrosa. Experimental Eye Research, 2022, 220, 109105.	1.2	1
6	Instant polarized light microscopy for imaging collagen microarchitecture and dynamics. Journal of Biophotonics, 2021, 14, e202000326.	1.1	16
7	Interplay between intraocular and intracranial pressure effects on the optic nerve head in vivo. Experimental Eye Research, 2021, 213, 108809.	1.2	13
8	A mesh-free approach to incorporate complex anisotropic and heterogeneous material properties into eye-specific finite element models. Computer Methods in Applied Mechanics and Engineering, 2020, 358, 112654.	3.4	24
9	Scleral structure and biomechanics. Progress in Retinal and Eye Research, 2020, 74, 100773.	7.3	153
10	Role of radially aligned scleral collagen fibers in optic nerve head biomechanics. Experimental Eye Research, 2020, 199, 108188.	1.2	16
11	So-Called Lamina Cribrosa Defects May Mitigate IOP-Induced Neural Tissue Insult. , 2020, 61, 15.		14
12	Connective tissue remodeling in myopia and its potential role in increasing risk of glaucoma. Current Opinion in Biomedical Engineering, 2020, 15, 40-50.	1.8	32
13	Lamina Cribrosa Capillaries Straighten as Intraocular Pressure Increases. , 2020, 61, 2.		12
14	Collagen fiber interweaving is central to sclera stiffness. Acta Biomaterialia, 2020, 113, 429-437.	4.1	36
15	Instant polarized light microscopy for real-time wide-field visualization of collagen architecture. , 2020, , .		2
16	A Mesh-Free Approach to Incorporate Complex Anisotropic and Heterogeneous Material Properties into Eye-Specific Finite Element Models. Computer Methods in Applied Mechanics and Engineering, 2020, 358, .	3.4	5
17	Polarized light microscopy for 3â€dimensional mapping of collagen fiber architecture in ocular tissues. Journal of Biophotonics, 2018, 11, e201700356.	1.1	46
18	Crimp around the globe; patterns of collagen crimp across the corneoscleral shell. Experimental Eye Research, 2018, 172, 159-170.	1.2	44

#	Article	IF	CITATIONS
19	Gaze-Evoked Deformations in Optic Nerve Head Drusen. Ophthalmology, 2018, 125, 929-937.	2.5	26
20	Collagen fiber recruitment: A microstructural basis for the nonlinear response of the posterior pole of the eye to increases in intraocular pressure. Acta Biomaterialia, 2018, 72, 295-305.	4.1	49
21	Thin Lamina Cribrosa Beams Have Different Collagen Microstructure Than Thick Beams. , 2018, 59, 4653.		17
22	Radial and Circumferential Collagen Fibers Are a Feature of the Peripapillary Sclera of Human, Monkey, Pig, Cow, Goat, and Sheep. , 2018, 59, 4763.		49
23	Seeing the Hidden Lamina: Effects of Exsanguination on the Optic Nerve Head. , 2018, 59, 2564.		7
24	Cerebrospinal Fluid Pressure: Revisiting Factors Influencing Optic Nerve Head Biomechanics. , 2018, 59, 154.		61
25	Tortuous Pore Path Through the Claucomatous Lamina Cribrosa. Scientific Reports, 2018, 8, 7281.	1.6	20
26	Peripapillary sclera architecture revisited: A tangential fiber model and its biomechanical implications. Acta Biomaterialia, 2018, 79, 113-122.	4.1	24
27	Spatial Patterns and Age-Related Changes of the Collagen Crimp in the Human Cornea and Sclera. , 2018, 59, 2987.		53
28	Structured polarized light microscopy for collagen fiber structure and orientation quantification in thick ocular tissues. Journal of Biomedical Optics, 2018, 23, 1.	1.4	20
29	Measuring in-vivo and in-situ ex-vivo the 3D deformation of the lamina cribrosa microstructure under elevated intraocular pressure. , 2018, , .		7
30	Effects of collagen microstructure and material properties on the deformation of the neural tissues of the lamina cribrosa. Acta Biomaterialia, 2017, 58, 278-290.	4.1	50
31	Whole-globe biomechanics using high-field MRI. Experimental Eye Research, 2017, 160, 85-95.	1.2	26
32	Location of the Central Retinal Vessel Trunk in the Laminar and Prelaminar Tissue of Healthy and Glaucomatous Eyes. Scientific Reports, 2017, 7, 9930.	1.6	11
33	Formalin Fixation and Cryosectioning Cause Only Minimal Changes in Shape or Size of Ocular Tissues. Scientific Reports, 2017, 7, 12065.	1.6	36
34	Collagen Architecture of the Posterior Pole: High-Resolution Wide Field of View Visualization and Analysis Using Polarized Light Microscopy. , 2017, 58, 735.		74
35	Lamina Cribrosa Pore Shape and Size as Predictors of Neural Tissue Mechanical Insult. , 2017, 58, 5336.		40
36	Thick Prelaminar Tissue Decreases Lamina Cribrosa Visibility. , 2017, 58, 1751.		12

Ian A Sigal

#	Article	IF	CITATIONS
37	Microstructural Crimp of the Lamina Cribrosa and Peripapillary Sclera Collagen Fibers. , 2017, 58, 3378-3388.		27
38	In-vivo effects of intraocular and intracranial pressures on the lamina cribrosa microstructure. PLoS ONE, 2017, 12, e0188302.	1.1	44
39	An imaged-based inverse finite element method to determine mechanical properties of the human trabecular meshwork. Journal for Modeling in Ophthalmology, 2017, 1, 100-111.	0.1	6
40	Use and Misuse of Laplace's Law in Ophthalmology. , 2016, 57, 236.		21
41	A Problem of Proportions in OCT-Based Morphometry and a Proposed Solution. , 2016, 57, 484.		19
42	Decreased Lamina Cribrosa Beam Thickness and Pore Diameter Relative to Distance From the Central Retinal Vessel Trunk. , 2016, 57, 3088.		10
43	Experimental Glaucoma Causes Optic Nerve Head Neural Rim Tissue Compression: A Potentially Important Mechanism of Axon Injury. , 2016, 57, 4403.		45
44	Regionally Discrete Aqueous Humor Outflow Quantification Using Fluorescein Canalograms. PLoS ONE, 2016, 11, e0151754.	1.1	44
45	MAPS – A Magic Angle Positioning System for Enhanced Imaging in High-Field Small-Bore MRI. Journal of Medical Robotics Research, 2016, 01, 1640004.	1.0	2
46	Identifying the Palisades of Vogt in Human ExÂVivo Tissue. Ocular Surface, 2016, 14, 435-439.	2.2	7
47	Non-invasive MRI Assessments of Tissue Microstructures and Macromolecules in the Eye upon Biomechanical or Biochemical Modulation. Scientific Reports, 2016, 6, 32080.	1.6	34
48	What is a typical optic nerve head?. Experimental Eye Research, 2016, 149, 40-47.	1.2	13
49	Histogram Matching Extends Acceptable Signal Strength Range on Optical Coherence Tomography Images. , 2015, 56, 3810.		13
50	In Vivo Evaluation of White Matter Integrity and Anterograde Transport in Visual System After Excitotoxic Retinal Injury With Multimodal MRI and OCT. , 2015, 56, 3788.		27
51	Translating Ocular Biomechanics into Clinical Practice: Current State and Future Prospects. Current Eye Research, 2015, 40, 1-18.	0.7	92
52	Polarization microscopy for characterizing fiber orientation of ocular tissues. Biomedical Optics Express, 2015, 6, 4705.	1.5	82
53	Gold Nanorods as a Contrast Agent for Doppler Optical Coherence Tomography. PLoS ONE, 2014, 9, e90690.	1.1	27
54	Reproducibility of In-Vivo OCT Measured Three-Dimensional Human Lamina Cribrosa Microarchitecture. PLoS ONE, 2014, 9, e95526.	1.1	24

#	Article	IF	CITATIONS
55	Eye-Specific IOP-Induced Displacements and Deformations of Human Lamina Cribrosa. , 2014, 55, 1.		121
56	In Vivo Three-Dimensional Characterization of the Healthy Human Lamina Cribrosa With Adaptive Optics Spectral-Domain Optical Coherence Tomography. , 2014, 55, 6459.		56
57	Recent advances in OCT imaging of the lamina cribrosa. British Journal of Ophthalmology, 2014, 98, ii34-ii39.	2.1	69
58	Characterisation of Schlemm's canal cross-sectional area. British Journal of Ophthalmology, 2014, 98, ii10-ii14.	2.1	31
59	Repeatability of in vivo 3D lamina cribrosa microarchitecture using adaptive optics spectral domain optical coherence tomography. Biomedical Optics Express, 2014, 5, 1114.	1.5	39
60	Parameters for Lithium Treatment Are Critical in Its Enhancement of Fracture-Healing in Rodents. Journal of Bone and Joint Surgery - Series A, 2014, 96, 1990-1998.	1.4	21
61	Magic Angle–Enhanced MRI of Fibrous Microstructures in Sclera and Cornea With and Without Intraocular Pressure Loading. , 2014, 55, 5662.		51
62	Automated lamina cribrosa microstructural segmentation in optical coherence tomography scans of healthy and glaucomatous eyes. Biomedical Optics Express, 2013, 4, 2596.	1.5	52
63	In Vivo Lamina Cribrosa Micro-Architecture in Healthy and Glaucomatous Eyes as Assessed by Optical Coherence Tomography. , 2013, 54, 8270.		86
64	Human Lamina Cribrosa Insertion and Age. , 2012, 53, 6870.		22
65	The Optic Nerve Head as a Robust Biomechanical System. , 2012, 53, 2658.		28
66	A Few Good Responses: Which Mechanical Effects of IOP on the ONH to Study?. , 2012, 53, 4270.		28
67	Lamina cribrosa thickening in early glaucoma predicted by a microstructure motivated growth and remodeling approach. Mechanics of Materials, 2012, 44, 99-109.	1.7	97
68	Glaucomatous cupping of the lamina cribrosa: A review of the evidence for active progressive remodeling as a mechanism. Experimental Eye Research, 2011, 93, 133-140.	1.2	199
69	Finite element modeling of the human sclera: Influence on optic nerve head biomechanics and connections with glaucoma. Experimental Eye Research, 2011, 93, 4-12.	1.2	163
70	3D visualization of aqueous humor outflow structures in-situ in humans. Experimental Eye Research, 2011, 93, 308-315.	1.2	67
71	Effect of Acute Intraocular Pressure Elevation on the Monkey Optic Nerve Head as Detected by Spectral Domain Optical Coherence Tomography. , 2011, 52, 9431.		118
72	Deformation of the Early Glaucomatous Monkey Optic Nerve Head Connective Tissue after Acute IOP Elevation in 3-D Histomorphometric Reconstructions. , 2011, 52, 345.		119

#	Article	IF	CITATIONS
73	Posterior (Outward) Migration of the Lamina Cribrosa and Early Cupping in Monkey Experimental Glaucoma. , 2011, 52, 7109.		159
74	IOP-Induced Lamina Cribrosa Displacement and Scleral Canal Expansion: An Analysis of Factor Interactions Using Parameterized Eye-Specific Models. , 2011, 52, 1896.		147
75	Longitudinal Change Detected by Spectral Domain Optical Coherence Tomography in the Optic Nerve Head and Peripapillary Retina in Experimental Glaucoma. , 2011, 52, 1206.		201
76	An Applet to Estimate the IOP-Induced Stress and Strain within the Optic Nerve Head. , 2011, 52, 5497.		21
77	IOP-Induced Lamina Cribrosa Deformation and Scleral Canal Expansion: Independent or Related?. , 2011, 52, 9023.		114
78	Mesh Morphing and Response Surface Analysis: Quantifying Sensitivity of Vertebral Mechanical Behavior. Annals of Biomedical Engineering, 2010, 38, 41-56.	1.3	15
79	Morphing methods to parameterize specimen-specific finite element model geometries. Journal of Biomechanics, 2010, 43, 254-262.	0.9	43
80	Correlation between Local Stress and Strain and Lamina Cribrosa Connective Tissue Volume Fraction in Normal Monkey Eyes. , 2010, 51, 295.		123
81	3D morphometry of the human optic nerve head. Experimental Eye Research, 2010, 90, 70-80.	1.2	87
82	Dimensions of the human sclera: Thickness measurement and regional changes with axial length. Experimental Eye Research, 2010, 90, 277-284.	1.2	179
83	A geometric morphometric assessment of the optic cup in glaucoma. Experimental Eye Research, 2010, 91, 405-414.	1.2	15
84	Changes in the Biomechanical Response of the Optic Nerve Head in Early Experimental Glaucoma. , 2010, 51, 5675.		93
85	Deformation of the Normal Monkey Optic Nerve Head Connective Tissue after Acute IOP Elevation within 3-D Histomorphometric Reconstructions. , 2009, 50, 5785.		115
86	Interactions between Geometry and Mechanical Properties on the Optic Nerve Head. , 2009, 50, 2785.		91
87	Modeling individual-specific human optic nerve head biomechanics. Part II: influence of material properties. Biomechanics and Modeling in Mechanobiology, 2009, 8, 99-109.	1.4	142
88	Modeling individual-specific human optic nerve head biomechanics. Part I: IOP-induced deformations and influence of geometry. Biomechanics and Modeling in Mechanobiology, 2009, 8, 85-98.	1.4	148
89	Biomechanics of the optic nerve head. Experimental Eye Research, 2009, 88, 799-807.	1.2	283
90	Mesh-morphing algorithms for specimen-specific finite element modeling. Journal of Biomechanics, 2008. 41. 1381-1389.	0.9	78

#	Article	IF	CITATIONS
91	Predicted extension, compression and shearing of optic nerve head tissues. Experimental Eye Research, 2007, 85, 312-322.	1.2	159
92	Factors Influencing Optic Nerve Head Biomechanics. , 2005, 46, 4189.		453
93	Reconstruction of human optic nerve heads for finite element modeling. Technology and Health Care, 2005, 13, 313-329.	0.5	69
94	Reconstruction of human optic nerve heads for finite element modeling. Technology and Health Care, 2005, 13, 313-29.	0.5	39
95	Finite Element Modeling of Optic Nerve Head Biomechanics. , 2004, 45, 4378.		286